Supporting Information

Pyrene spiropyran diyad: solvato-, acido- and mechanofluorochromic properties and its application in acid sensing and reversible fluorescent display

Xing Su, [a,b] *Yanglimin Ji,* [a] *Wanting Pan,* [a] *Siqi Chen,* [a] *Yu-Mo Zhang,* [a] *Tingting Lin,*

[*b] *Lulu Liu,* [a] *Minjie Li,* [c] *Yifei Liu,*[*a] *Sean Xiao-An Zhang* [c]

[a] College of Chemistry, Jilin University, Changchun 130012, China.

[b] College of Instrumentation and Electrical Engineering. Jilin University, Changchun, 130061, P. R. China.

[c] State Key Lab of Supramolecular Structure and Materials, College of Chemistry,

Jilin University, Changchun 130012, China.

Table S1 The emission wavelength, absorption wavelength and ΔE between HOMO and LUMO of Py-Sp in various solutions.

Solvent	Em (nm)	Abs (nm)	ΔE(eV)
Hexane	418	352	3.5253
Toluene	439	355	3.5188
$CHCl_3$	457	358	3.5033
EtOAc	460	353	3.5014
THF	462	354	3.4989
EtOH	468	355	3.4903
DCM	470	355	3.4973
MeOH	479	351	3.4910
MeCN	494	353	3.4908
DMF	497	357	3.4892
DMSO	502	358	3.4900

Table. S2 The CIE coordinates of PYSP in different solvents.

Solvent	CIE coordinate
Hexane	(0.1603, 0.0375)
Toluene	(0.1527, 0.0606)
$CHCl_3$	(0.1437, 0.1171)
EtOAc	(0.1445, 0.1329)
THF	(0.1435, 0.1409)
EtOH	(0.1486, 0.1917)
DCM	(0.1437, 0.1966)
MeOH	(0.1601, 0.2611)
MeCN	(0.1877, 0.3775)
DMF	(0.1872, 0.3863)
DMSO	(0.2124, 0.4416)

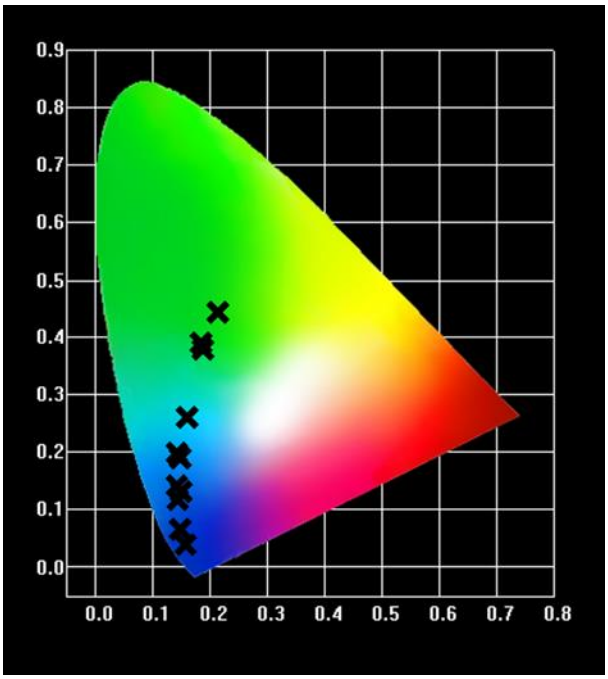

Fig. S1 CIE graph of Py-Sp in different solvents.

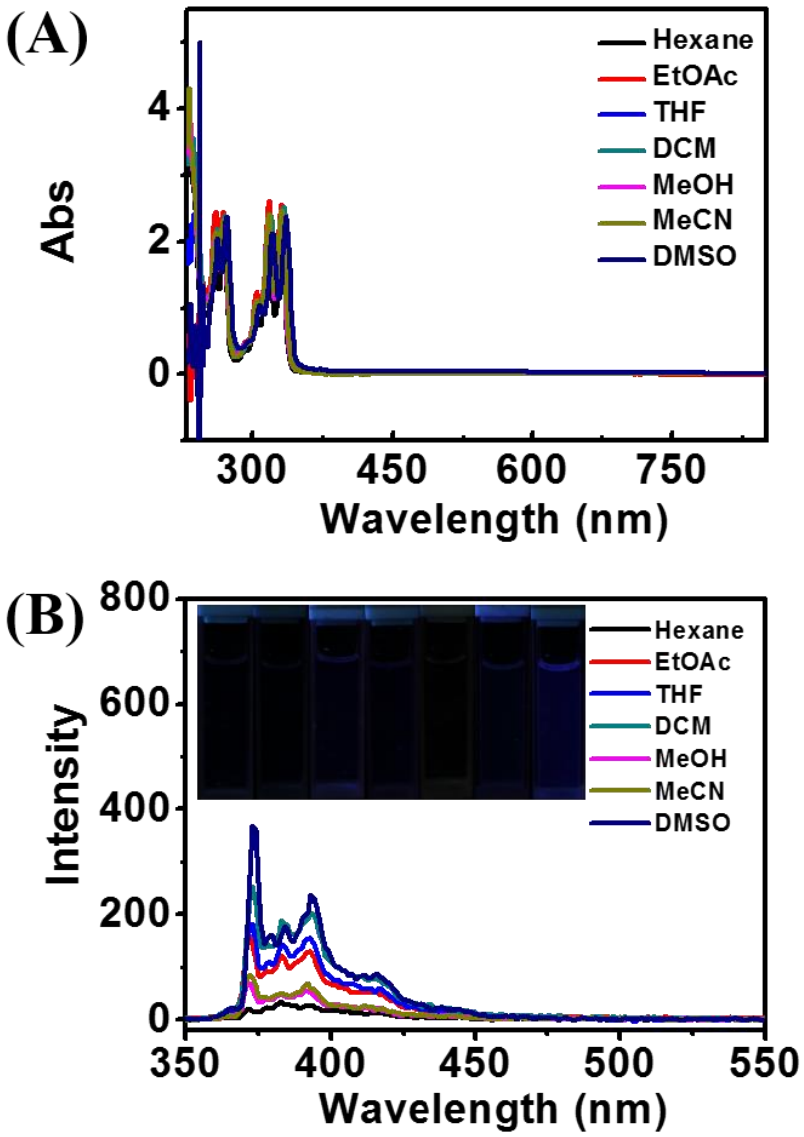

Fig. S2 (A) The absorption spectra and (B) PL spectra of pyrene in different solutions (1×10^{-4} M). Insets are the fluorescent pictures taken under 365 nm UV light.

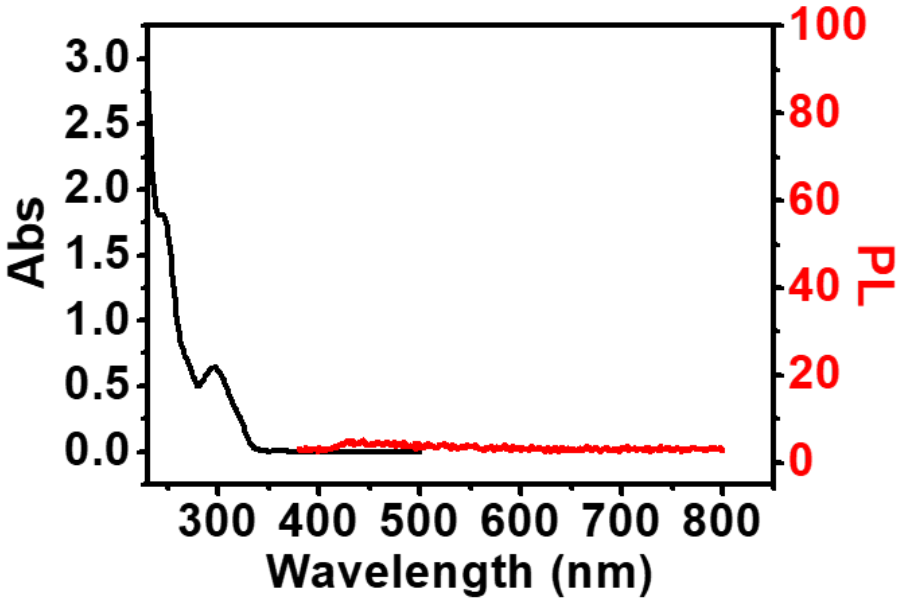

Fig. S3 The absorption and PL spectra of spiropyran in acetonitrile (1×10^{-4} M).

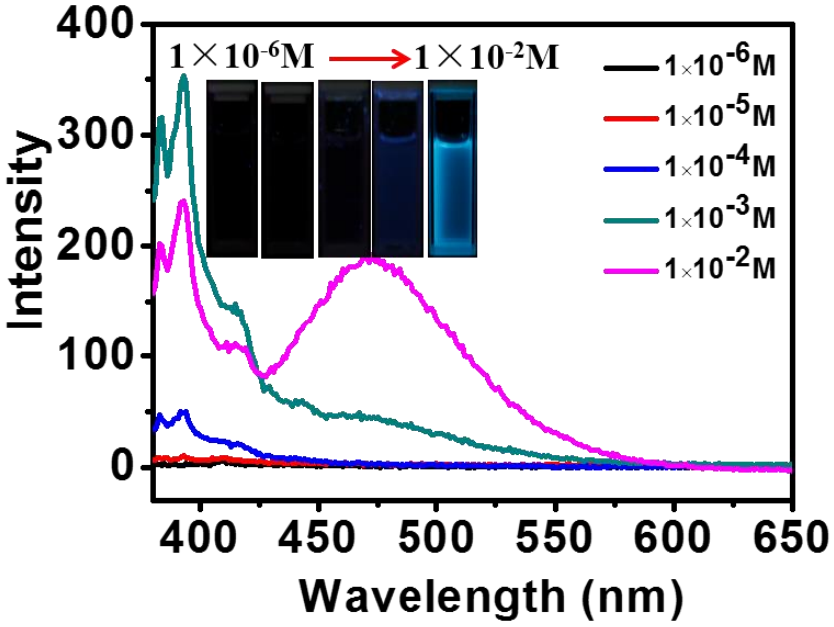

Fig. S4 The PL spectra of pyrene in THF solution with concentration increasing from 1×10^{-6} M to 1×10^{-2} M. Insets are the fluorescent pictures taken under 365 nm UV light.

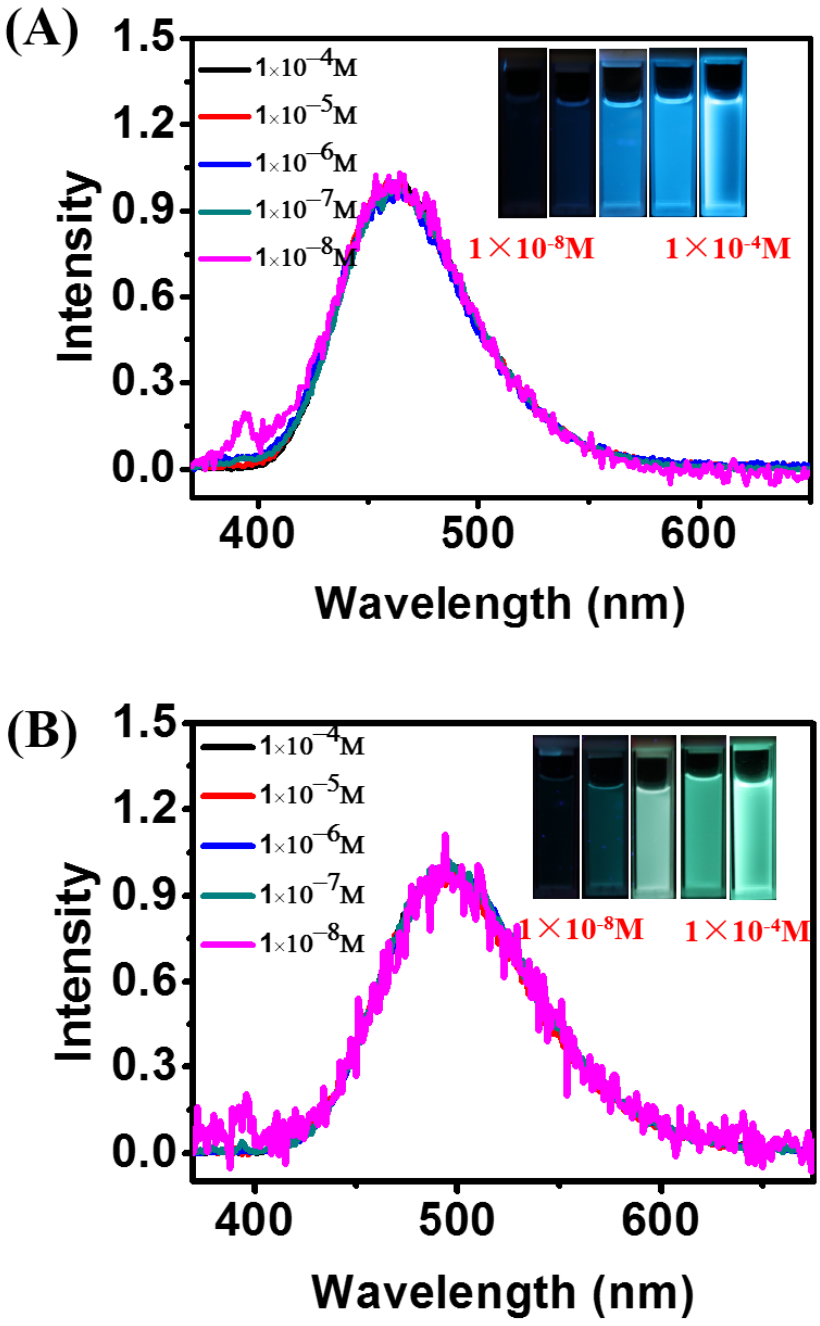

Fig. S5 The PL spectra of Py-Sp in (A) THF solution and (B) MeCN solution with concentration from 1×10^{-8} M to 1×10^{-4} M.

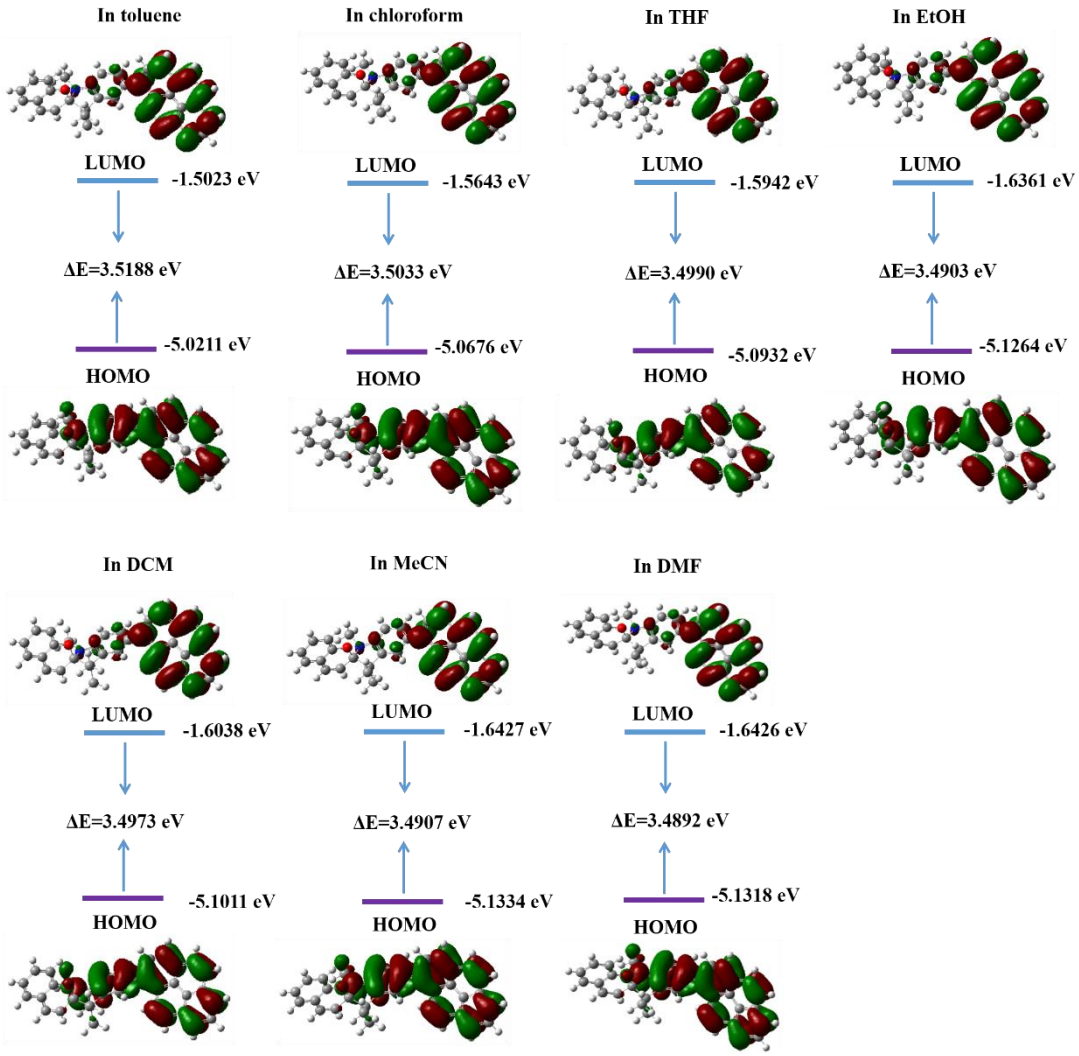

Fig. S6 The spatial electron distribution of HOMOs and LUMOs of Py-Sp in toluene, chloroform, THF, EtOH, DCM, MeCN and DMF solution, which were calculated by Gaussian 09 with B3LYP/6-31G(d).

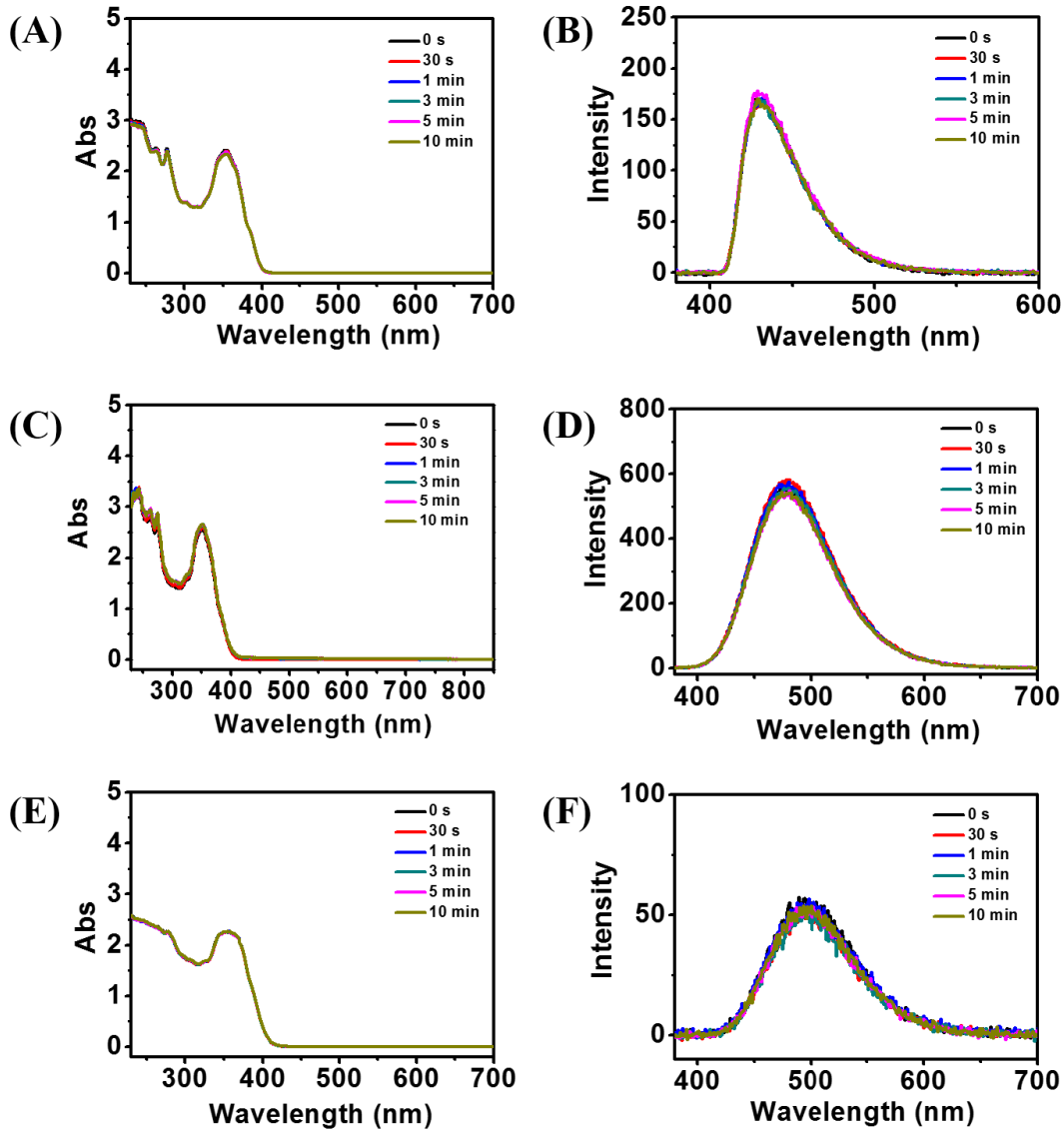

Fig.S7 (A), (C), (E) The absorption spectra and (B), (D), (F) the PL spectra of Py-Sp in n-hexane, methanol and acetonitrile after treated with different time of 254 nm UV light irradiation.

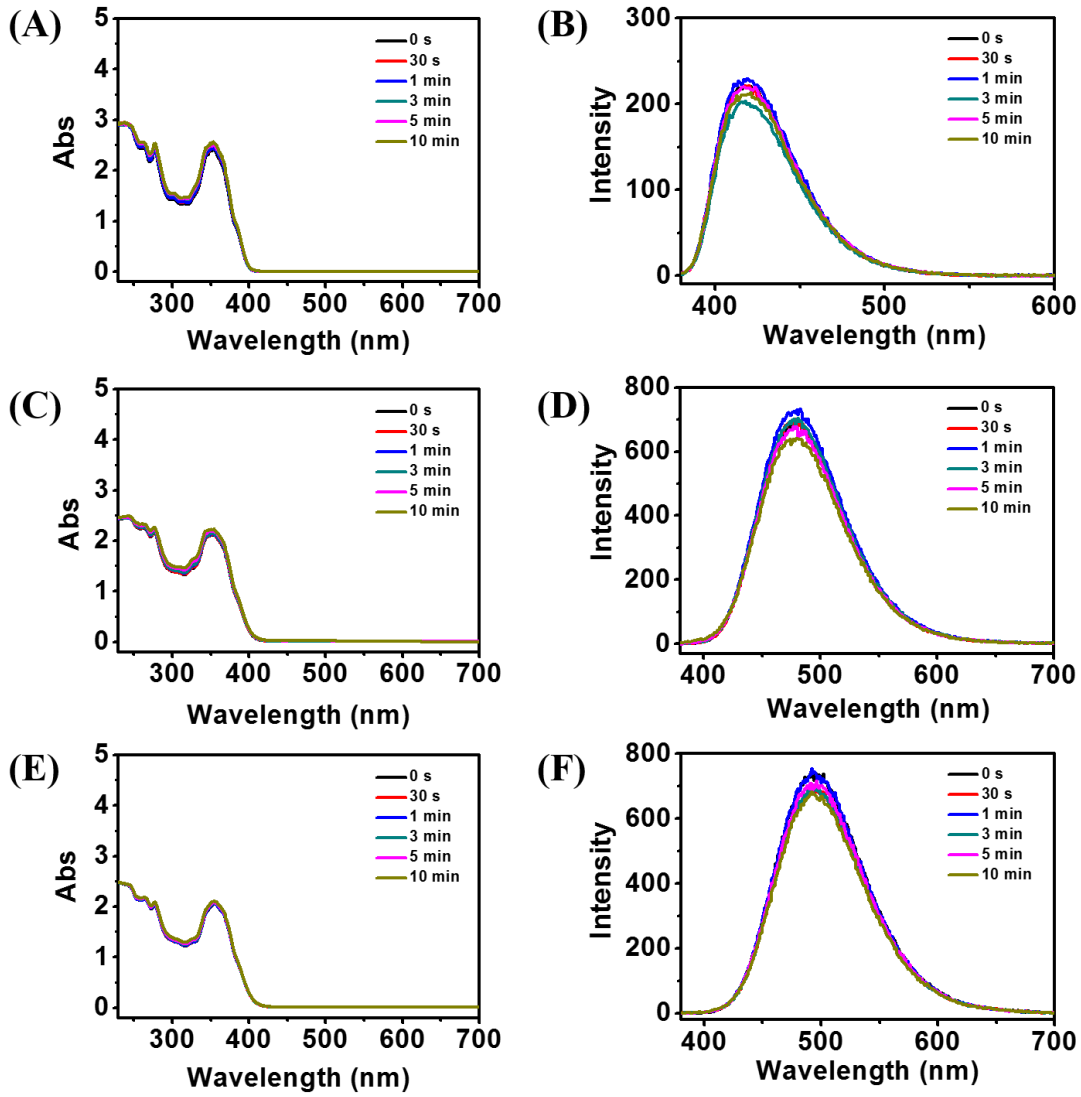

Fig.S8 (A), (C), (E) The absorption spectra and (B), (D), (F) the PL spectra of Py-Sp in n-hexane, methanol and acetonitrile after treated with different time of 365 nm UV light irradiation.

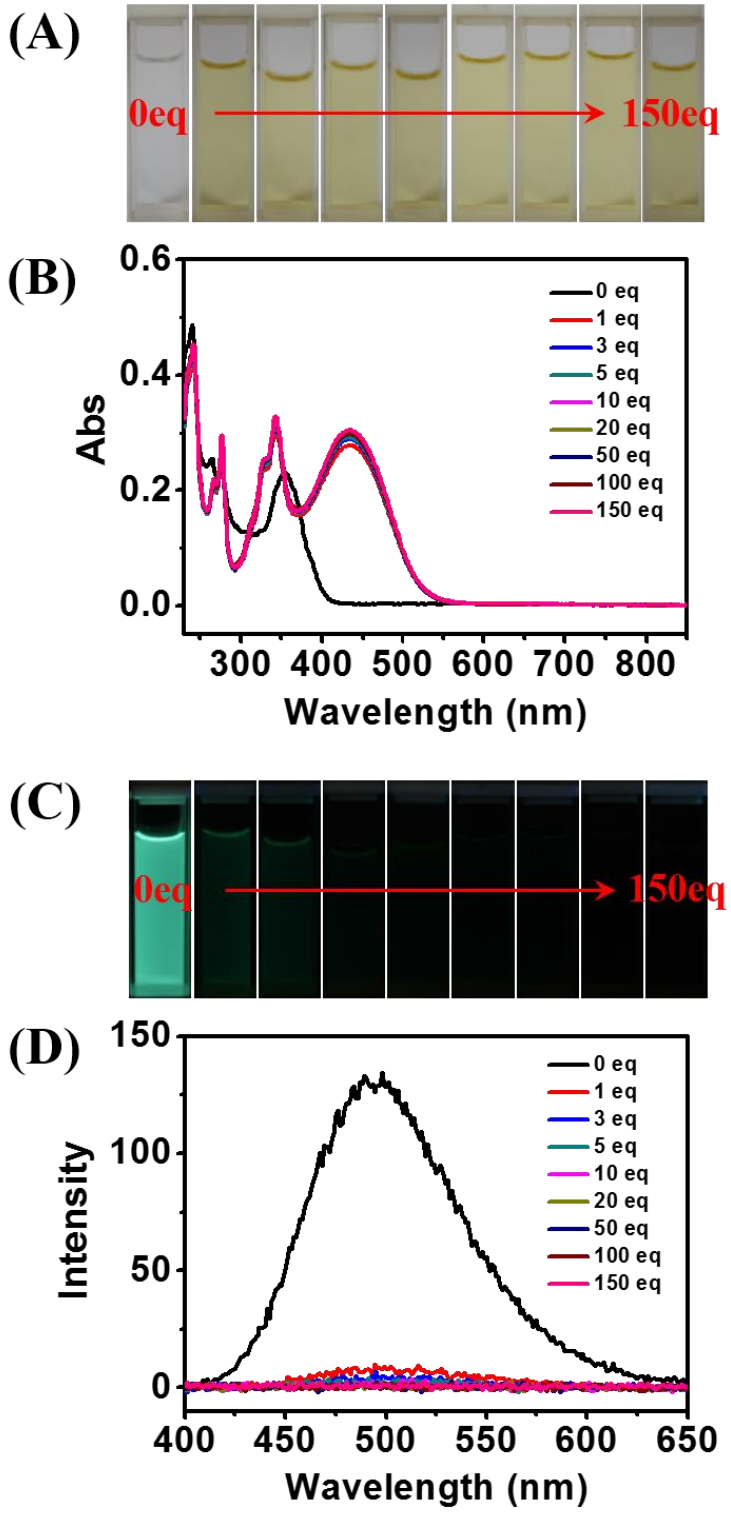

Fig.S9 (A) The pictures and (C) fluorescent images of Py-Sp in acetonitrile solution (1×10^{-5} M) after treated with different equivalents of HCl. (B) The absorption spectra and (D) PL spectra of the corresponding solutions.

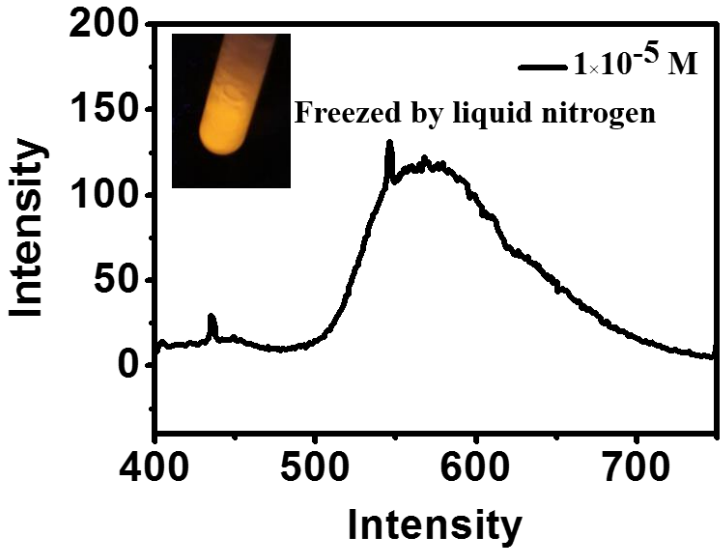

Fig. S10 The PL spectrum of Py-MCH ethanol solution (1×10^{-5} M) frozen in liquid nitrogen. Inset is the corresponding fluorescent image taken under 365 nm UV light.

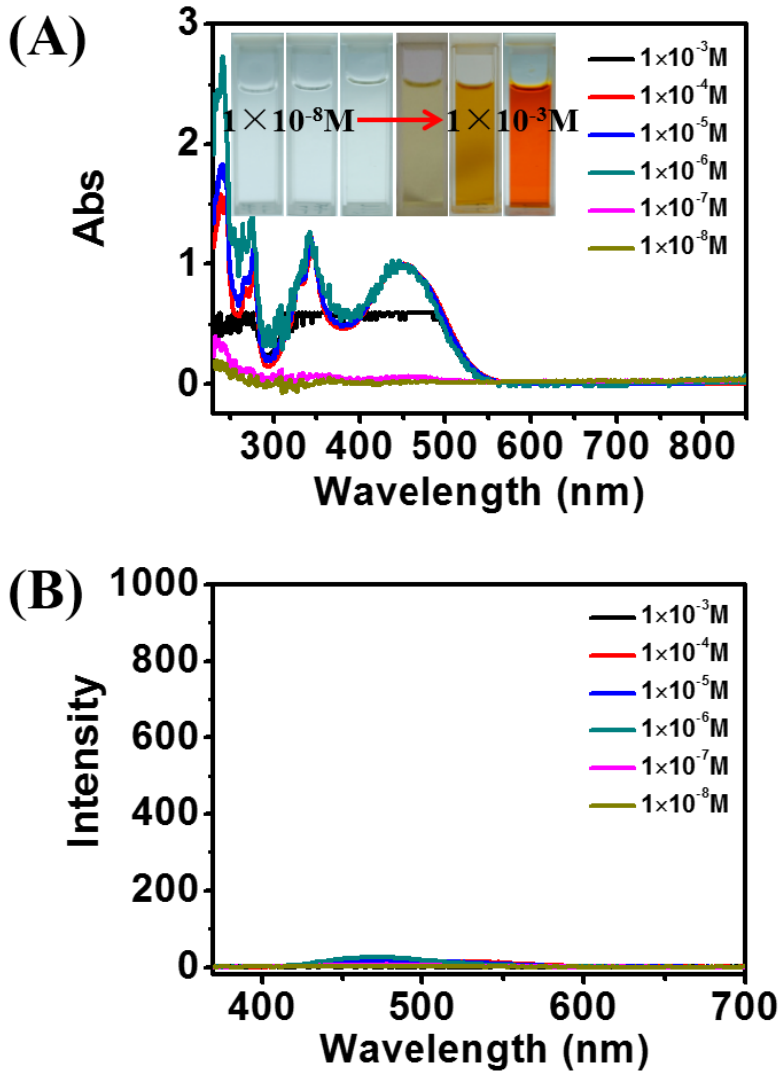

Fig. S11 (A) The absorption spectra and (B) PL spectra of Py-Sp ethanol solution with different concentrations. When the concentration is higher than 1×10^{-5} M, the acid equivalent is 500, while the concentration of Py-Sp is lower than 1×10^{-5} M, the acid concentration is fixed at 5×10^{-3} M to ensure the complete conversion from Py-Sp to Py-MCH. Insets are the pictures of Py-MCH solution with different concentrations.

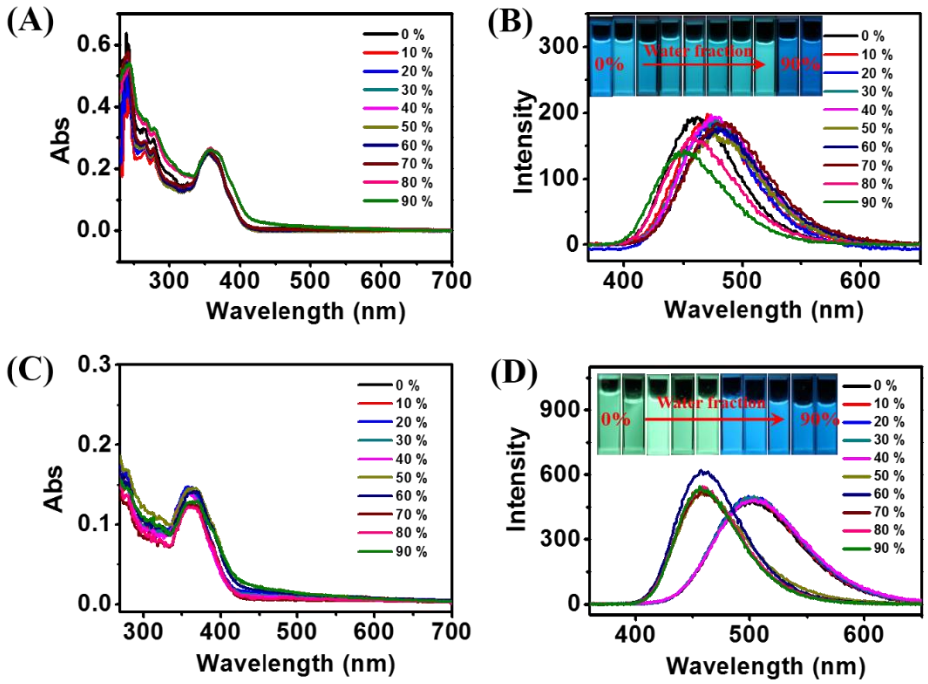

Fig. S12 (A) The absorption spectra and (B) the PL spectra of Py-Sp in different volume fraction of water/THF mixtures (1×10^{-5} M). (C) The absorption spectra and (D) the PL spectra of Py-Sp in different volume fraction of water/DMSO mixtures (1×10^{-5} M).

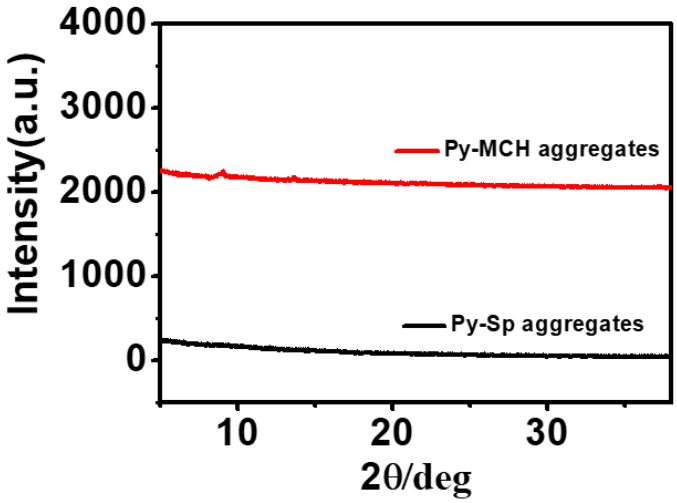

Fig. S13 The XRD patterns of Py-Sp and Py-MCH aggregates.

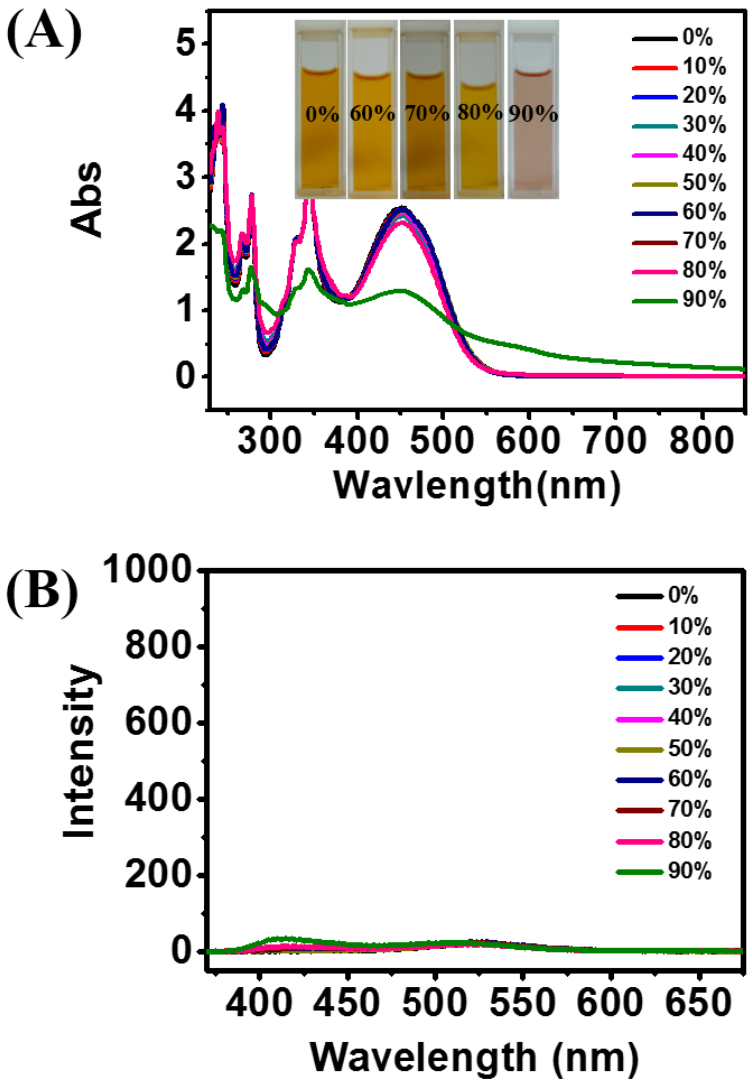

Fig. S14 (A) The absorption spectra and (B) the PL spectra of Py-Sp (1×10^{-4} M) with 500 equivalents of HCl in different volume fraction of n-hexane/ethanol mixtures.

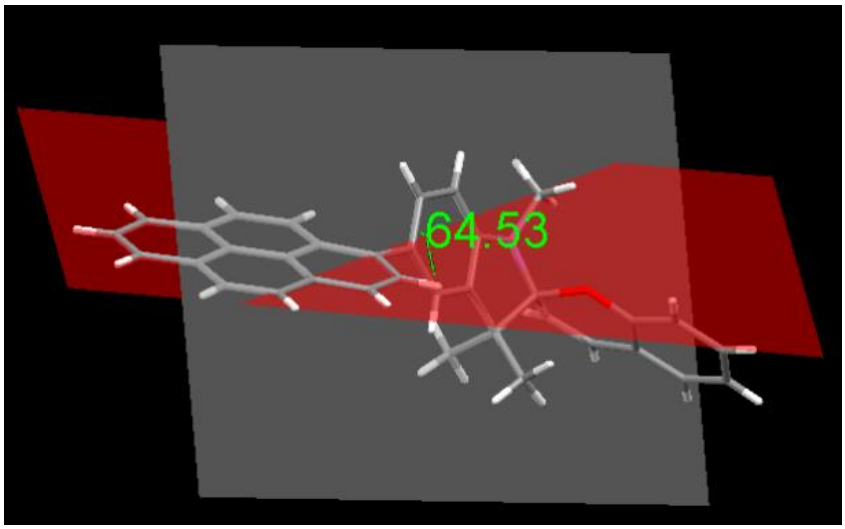

Fig. S15 The dihedral angle between pyrene and indole planes in single crystal.

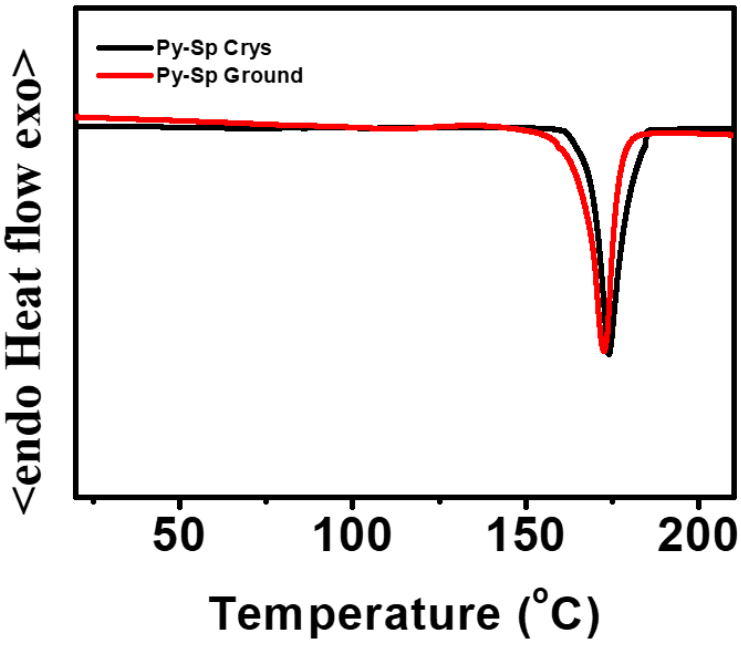

Fig.S16 The DSC curves of Py-Sp crystals before and after grinding.

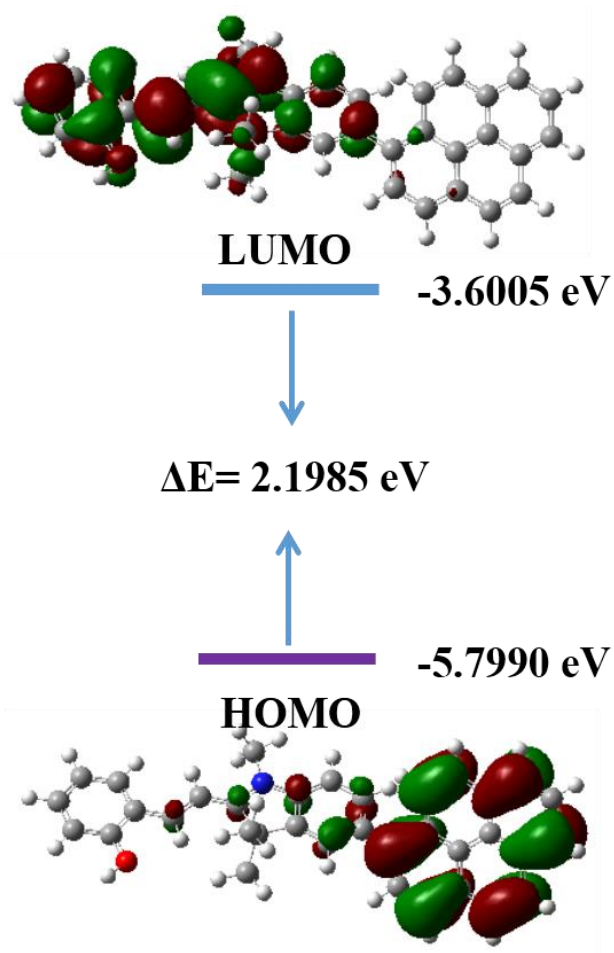

Fig. S17 The spatial electron distribution of HOMO and LUMO of Py-MCH in optimized state, which was calculated by Gaussian 09 with B3LYP/6-31G(d).

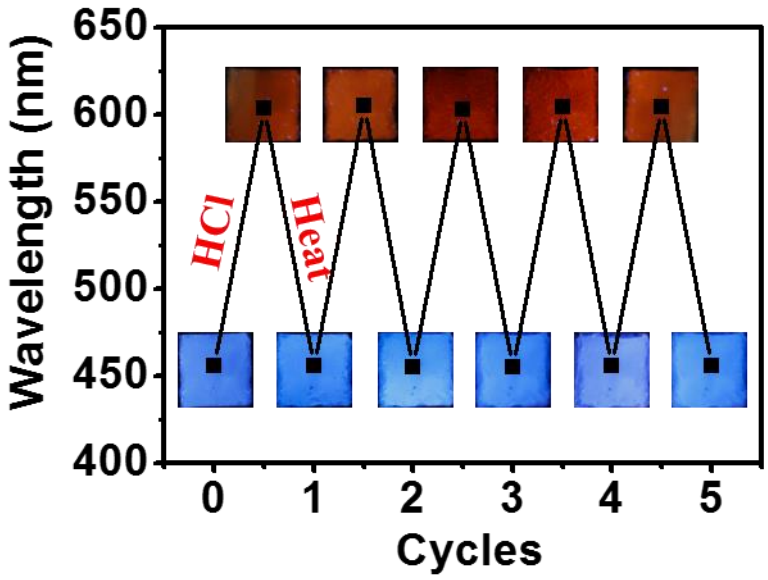

Fig. S18 The wavelength contrast profiles of Py-Sp/PVP coating under HCl and heat treatment with switching cycles.

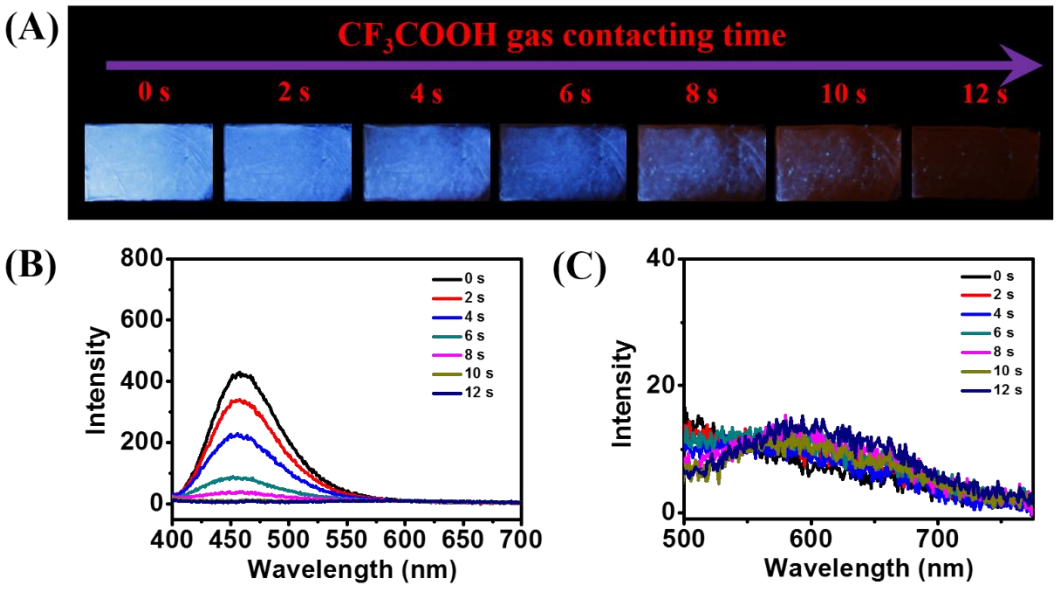

Fig. S19 The fluorescent pictures (A) and PL spectra (B, Ex:390 nm; C, Ex:440 nm) of Py-Sp/PVP electrospinning nanofiber film exposure to saturated CF_3COOH gas with different time.

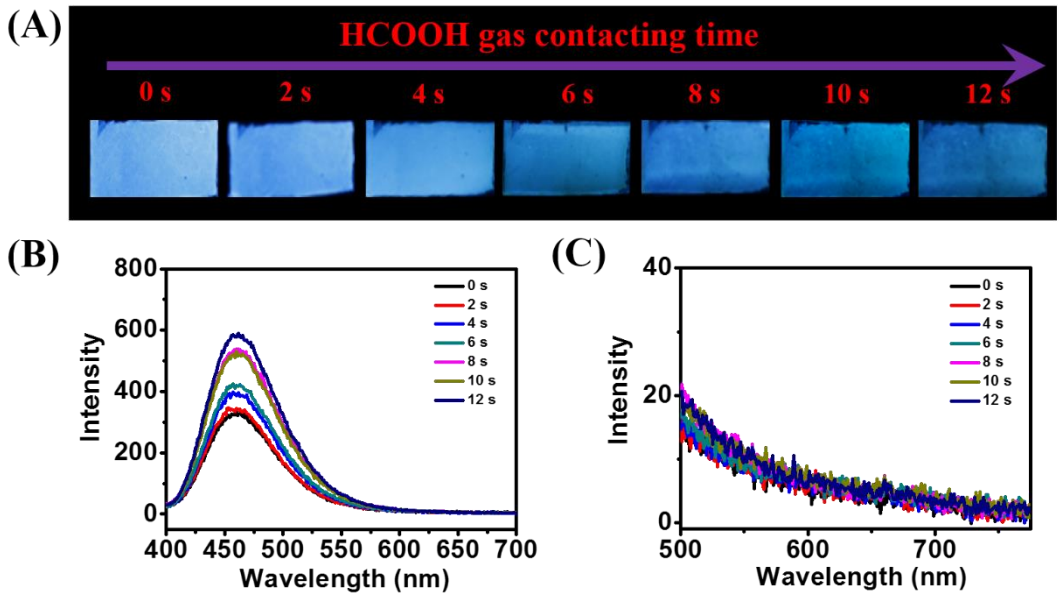

Fig. S20 The fluorescent pictures (A) and PL spectra (B, Ex:390 nm; C, Ex:440 nm) of Py-Sp/PVP electrospinning nanofiber film exposure to saturated HCOOH gas with different time.

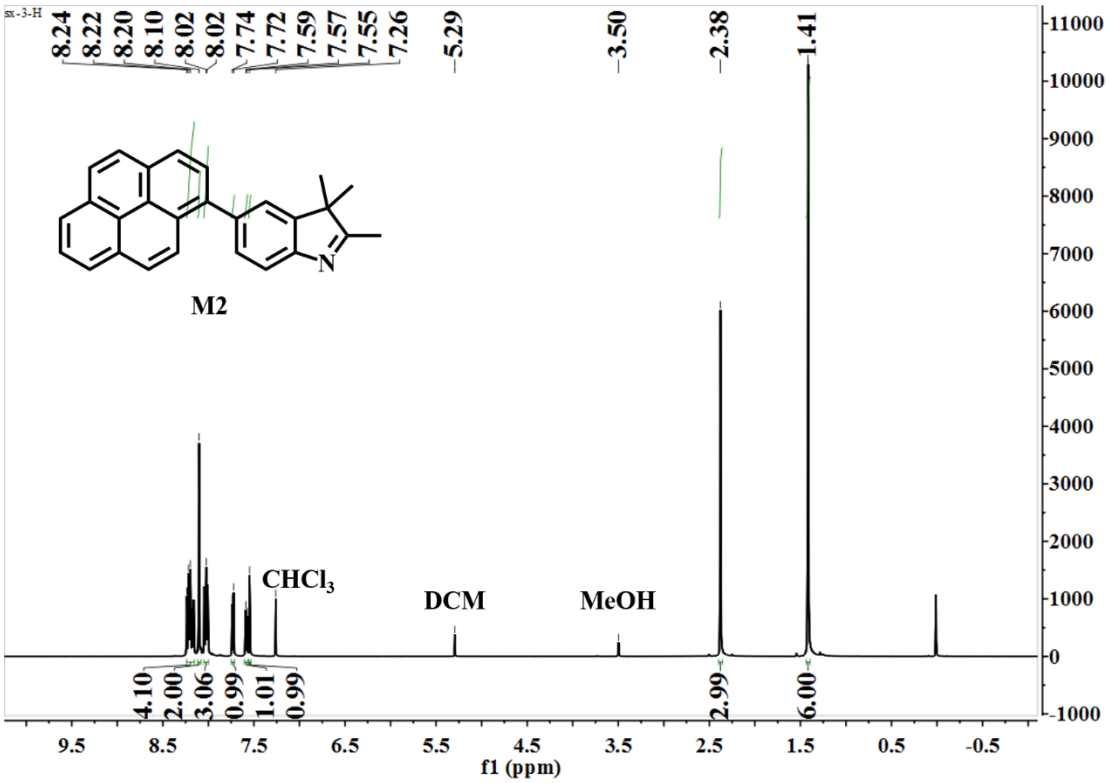

Fig. S21 ^{1}H NMR spectrum of **M2** in $CDCl_3$.

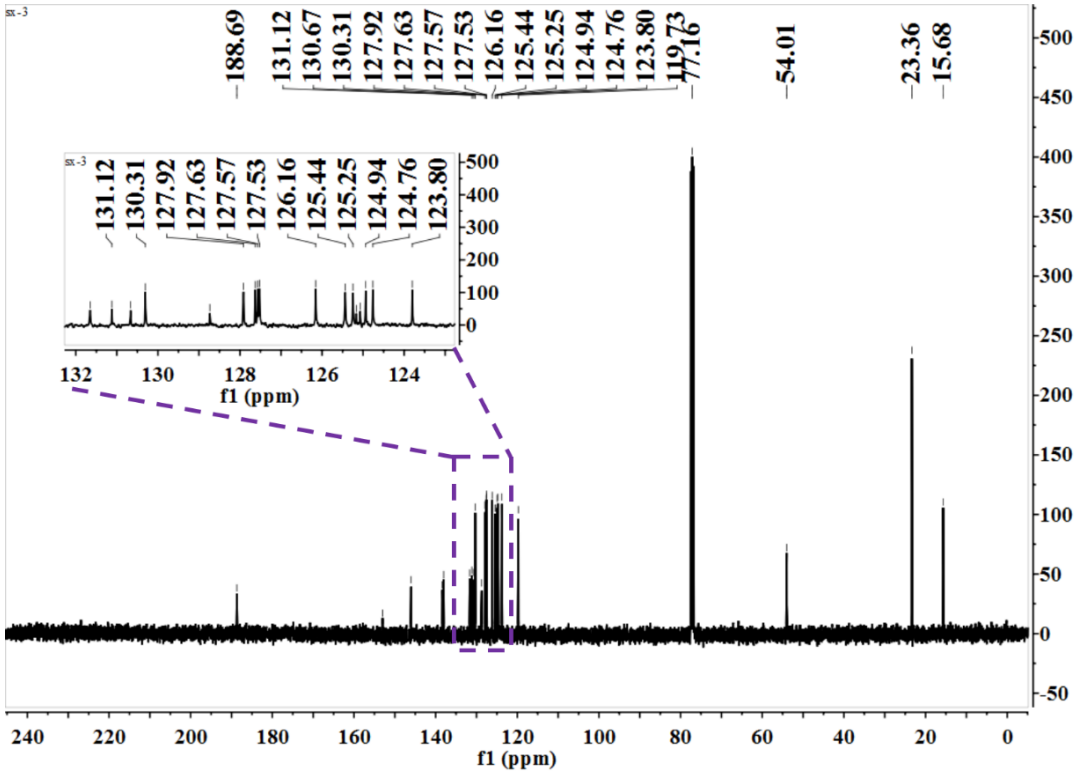

Fig. S22 ^{13}C NMR spectrum of **M2** in $CDCl_3$.

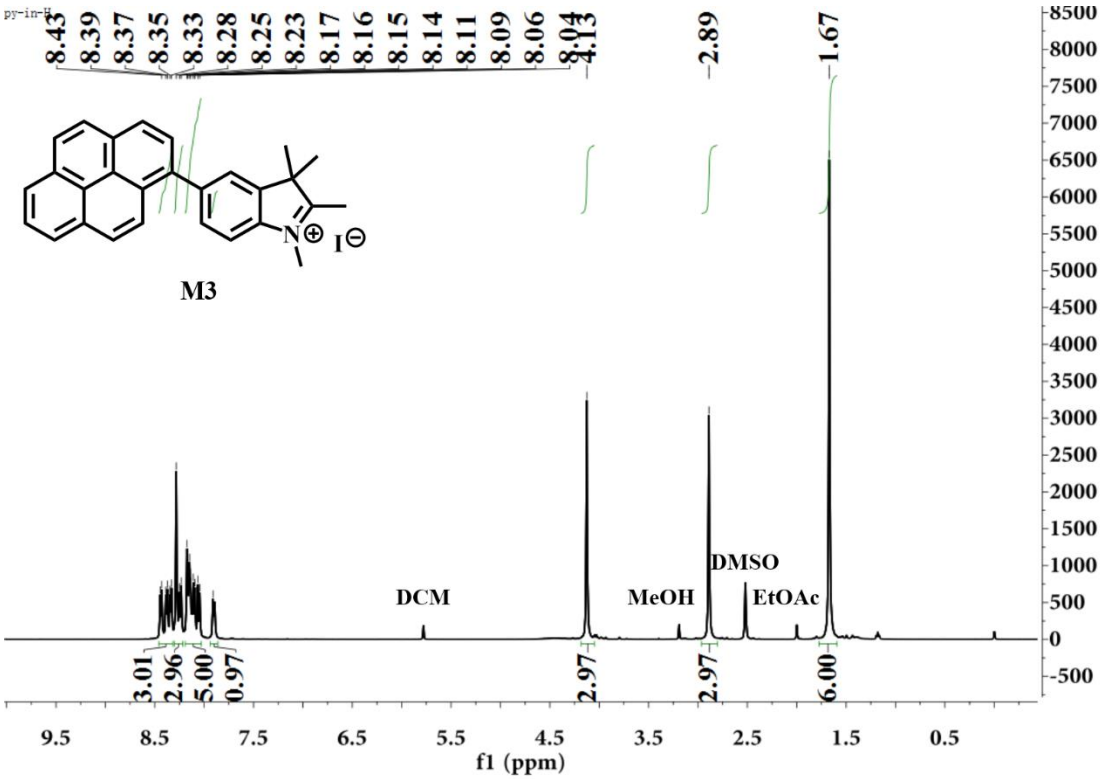

Fig. S23 ^{1}H NMR spectrum of **M3** in d_6-DMSO.

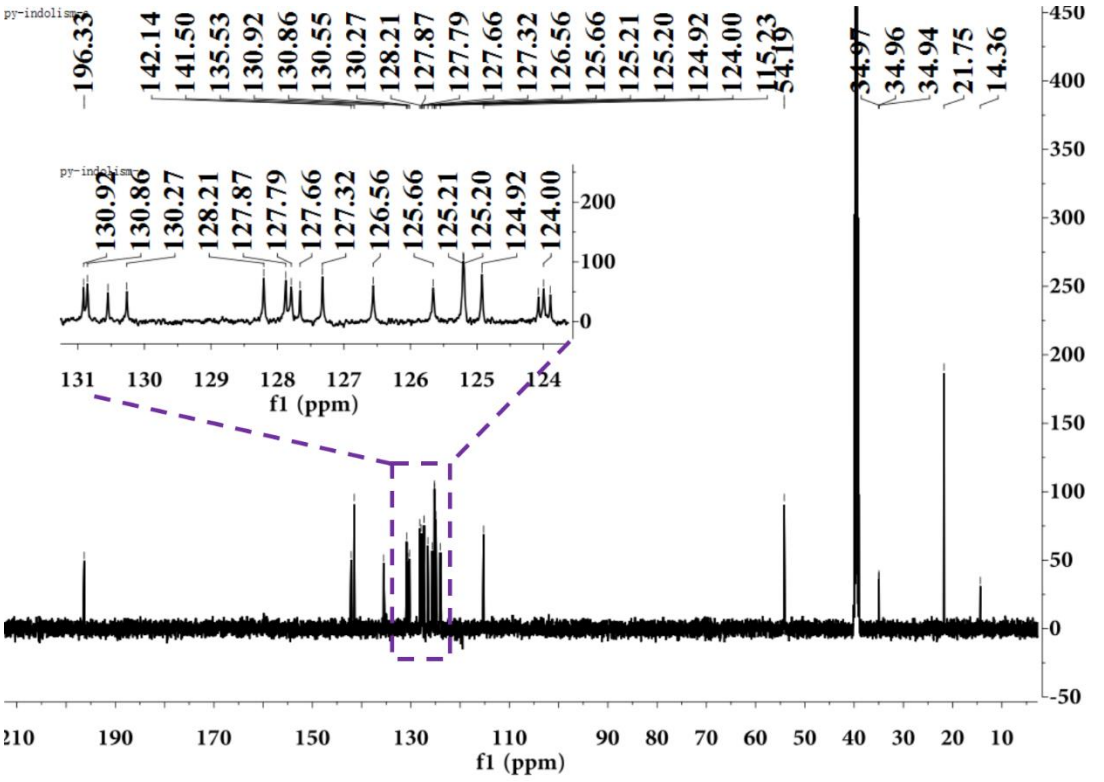

Fig. S24 ^{13}C NMR spectrum of **M3** in d_6-DMSO.

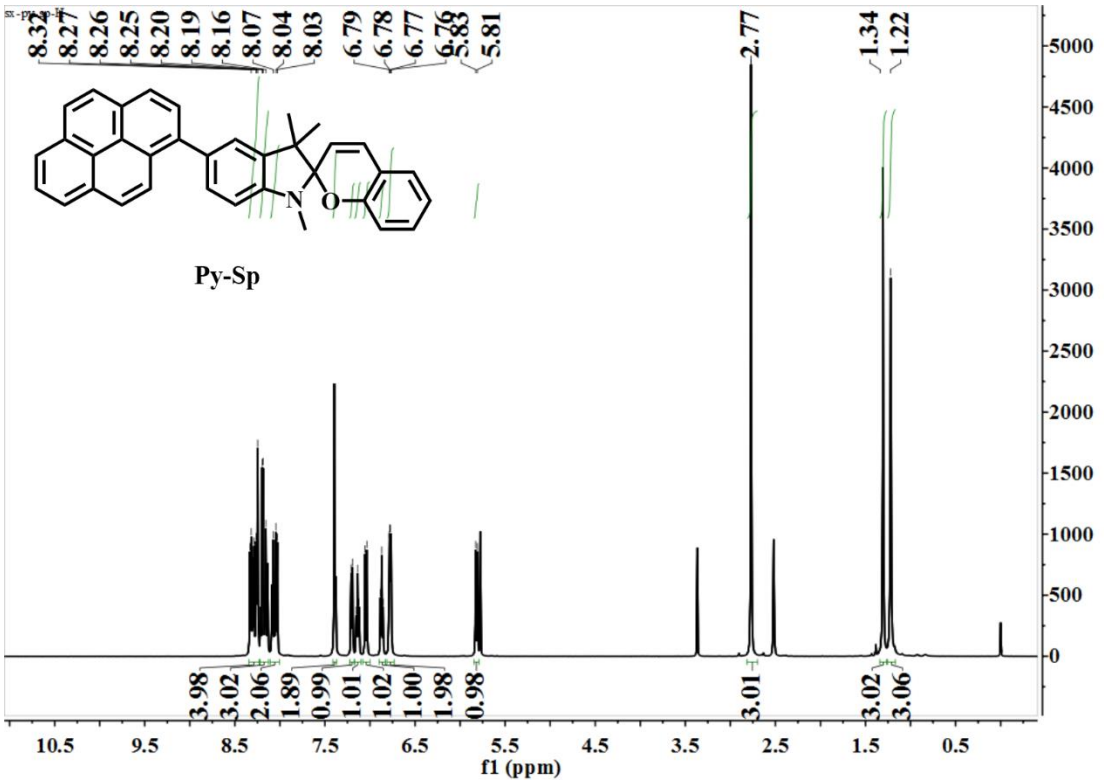

Fig. S25 ^{1}H NMR spectrum of **Py-Sp** in d_6-DMSO.

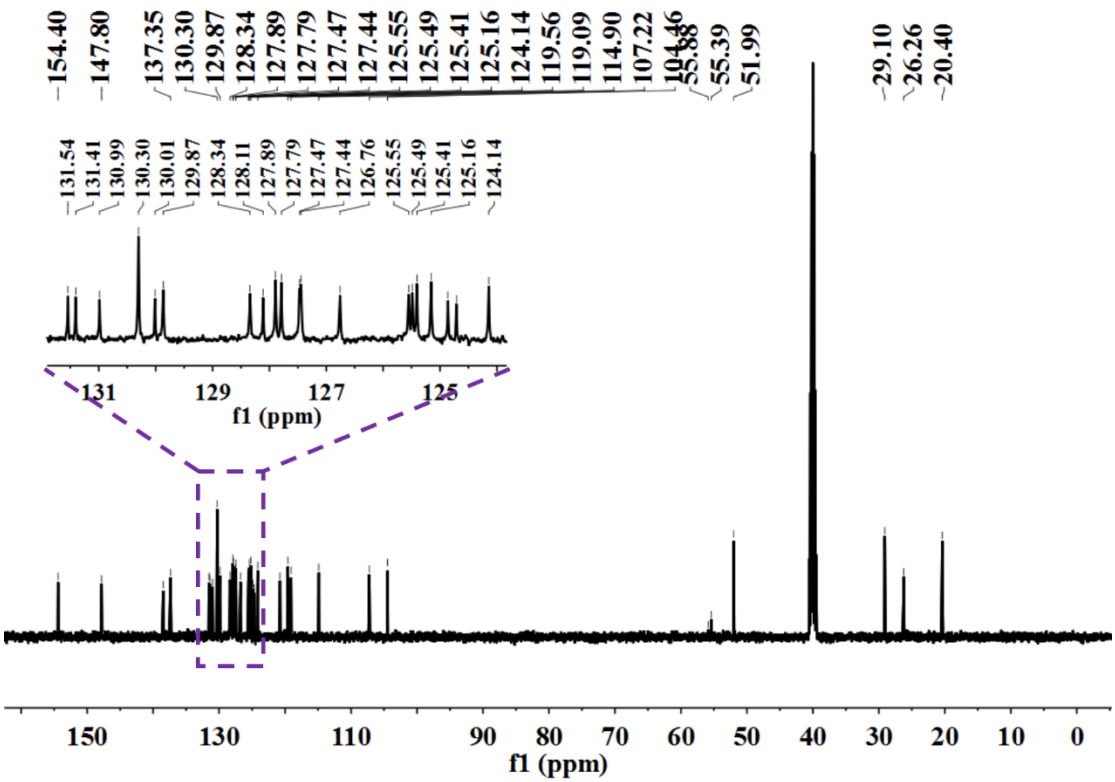

Fig. S26 ^{13}C NMR spectrum of **Py-Sp** in d_6-DMSO.

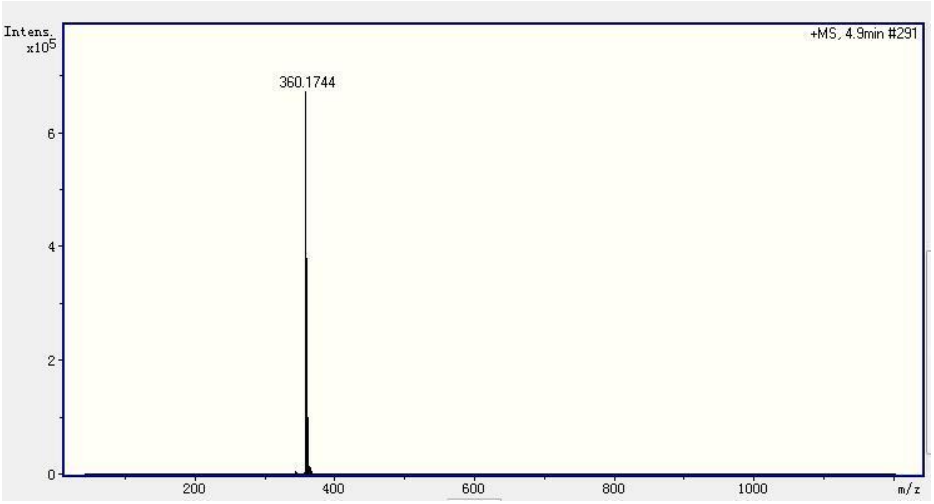

Fig. S27 The MS spectra of **M2**.

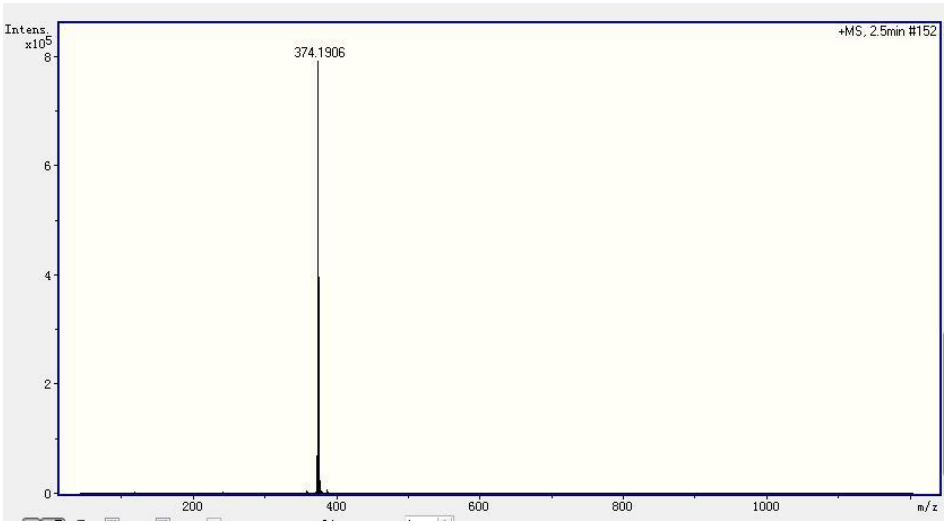

Fig. S28 The MS spectra of **M3**.

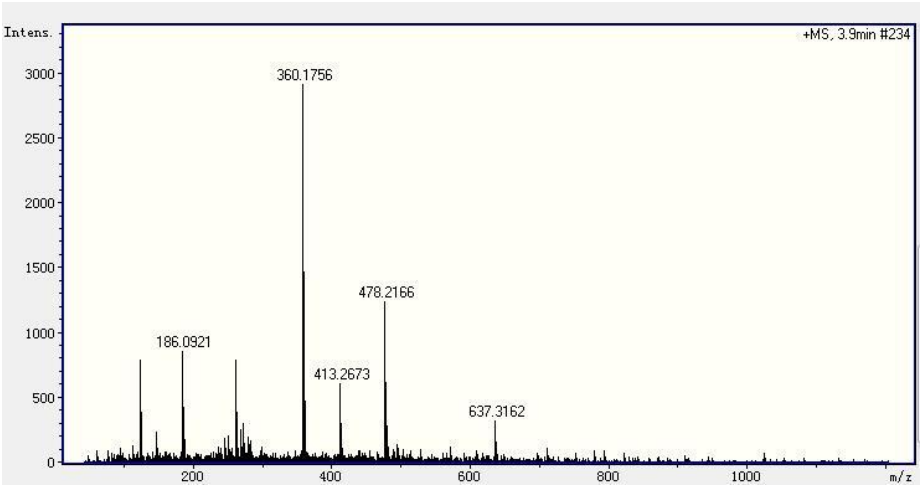

Fig. S29 The MS spectra of **Py-Sp**.